

## Tracking Dark Excitons with Exciton Polaritons in Semiconductor Microcavities

D. Schmidt,<sup>1</sup> B. Berger,<sup>1</sup> M. Kahlert,<sup>1</sup> M. Bayer,<sup>1,2</sup> C. Schneider,<sup>3</sup> S. Höfling,<sup>3,4</sup> E. S. Sedov,<sup>5,6</sup>  
A. V. Kavokin,<sup>7,8</sup> and M. Aßmann<sup>1</sup>

<sup>1</sup>*Experimentelle Physik 2, Technische Universität Dortmund, D-44221 Dortmund, Germany*

<sup>2</sup>*A. F. Ioffe Physical-Technical Institute, Russian Academy of Sciences, St. Petersburg 194021, Russia*

<sup>3</sup>*Technische Physik, Universität Würzburg, 97074 Würzburg, Germany*

<sup>4</sup>*SUPA, School of Physics and Astronomy, University of St. Andrews, St. Andrews KY16 9SS, United Kingdom*

<sup>5</sup>*School of Physics and Astronomy, University of Southampton, SO17 1NJ Southampton, United Kingdom*

<sup>6</sup>*Vladimir State University named after A. G. and N. G. Stoletovs, Gorky Street 87, 600000, Vladimir, Russia*

<sup>7</sup>*Spin Optics Laboratory, St. Petersburg State University, Ulanovskaya 1, Peterhof, St. Petersburg 198504, Russia*

<sup>8</sup>*International Center for Polaritonics, Westlake University,  
No. 18, Shilongshan Road, Cloud Town, Xihu District, Hangzhou, China*



(Received 2 July 2018; revised manuscript received 30 October 2018; published 1 February 2019)

Dark excitons are of fundamental importance for a wide variety of processes in semiconductors but are difficult to investigate using optical techniques due to their weak interaction with light fields. We reveal and characterize dark excitons nonresonantly injected into a semiconductor microcavity structure containing InGaAs/GaAs quantum wells by a gated train of eight 100 fs pulses separated by 13 ns by monitoring their interactions with the bright lower polariton mode. We find a surprisingly long dark exciton lifetime of more than 20 ns, which is longer than the time delay between two consecutive pulses. This creates a memory effect that we clearly observe through the variation of the time-resolved transmission signal. We propose a rate equation model that provides a quantitative agreement with the experimental data.

DOI: 10.1103/PhysRevLett.122.047403

A detailed understanding of the nature of electronic excitations in semiconductor crystals is fundamental in order to explain their dynamics, collective interactions, and many-body effects. Optical spectroscopy provides a convenient range of characterization tools for those excitations that are bright, which means that they can absorb or emit light. It is much more complicated to gain experimental access to optically inactive or dark excitations which interact weakly or not at all with light. So-called dark excitons are typical representatives of such excitations. Still, their properties are decisive for a wide range of systems ranging from semiconductor monolayers [1–3] and light-harvesting complexes [4] to quantum dots [5–7], where dark excitons form an essential building block for the generation of on-demand entangled photon cluster states [8].

Here, we demonstrate that a quasiresonantly driven microcavity polariton condensate is a sensitive probe for the presence of dark excitons, and, vice versa, dark excitons can be utilized to introduce long-lived potentials for a polariton system. Microcavity exciton polaritons are composite quasiparticles resulting from the strong coupling of photons and bright excitons in a microcavity structure containing embedded quantum wells. They are known to exhibit several kinds of bistability [9–12] or multistability [13,14], most prominently in the transmission curve when probed quasiresonantly at an energy slightly above the lower polariton branch using a narrow cw laser [15].

We first realize this kind of polariton bistability using the following setup: The sample is a planar GaAs  $\lambda$  cavity consisting of 26 top and 30 bottom GaAs/AlAs distributed Bragg reflector layer pairs, containing six In<sub>0.1</sub>Ga<sub>0.9</sub>As quantum wells placed at the central antinodes of the confined light field. The sample shows a Rabi splitting of about 6 meV and is mounted on the ring-shaped cold finger of a continuous flow helium cryostat at a temperature of 14.8 K. The measurements are performed at a positive detuning of 1.8 meV between the cavity and the exciton mode. The linearly polarized cw probe beam is provided by an M-Squared SolsTis cw Ti:sapphire laser with a linewidth below 100 kHz. The laser beam is focused to a spot diameter of about 40  $\mu\text{m}$  onto the sample at normal incidence at a detuning of 650  $\mu\text{eV}$  with respect to the empty cavity lower polariton mode, which shows a linewidth of about 170  $\mu\text{eV}$ . The light transmitted through the cavity is detected using a 400 MHz bandwidth photodiode.

Figure 1(a) demonstrates the measured hysteresis cycle of the transmission through the sample showing stable off and on states and a bistable region in between, which is a consequence of the repulsive interaction of polaritons with the same spin [16]. Accordingly, the lower polariton mode experiences a spectral blueshift that depends on the polariton occupation number. Thus, it is the spectral overlap between the lower polariton mode and the probe beam that governs the transmission of the latter through the cavity.

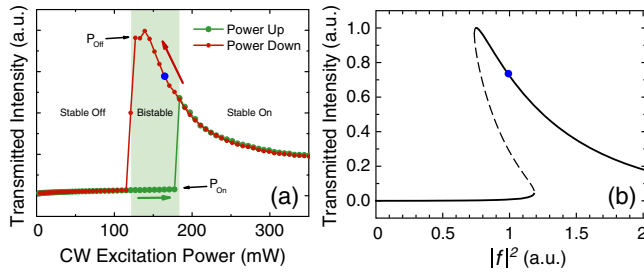


FIG. 1. (a) Measured transmission intensity through the sample as a function of the cw excitation pump power. (b) Transmission through the structure simulated using Eqs. (1) and (2). Blue circles denote the working position for further discussion.

The presence of other carriers will also introduce a shift of the polariton mode [17–20]. As this shift directly translates to a modified probe beam transmission, the latter becomes a sensitive tool to detect the presence of other carriers and measure the strength of their interactions.

Next, we introduce additional carriers into the system and monitor their dynamics using the setup just presented. To this end, we employ a pulsed Ti:sapphire laser with a pulse repetition rate of 75.39 MHz and a pulse duration of about 100 fs to perform far off-resonant excitation at the center of the fourth Bragg minimum of the microcavity structure at 737 nm. The off-resonant pump is focused to the same sample position as the probe laser but has a larger diameter of 75  $\mu\text{m}$  to ensure that the probe laser samples only the central region of the pump spot. It should be noted that the sample does not show spontaneous condensation under nonresonant excitation. A transition into the weak coupling regime will occur at some point, but all pump powers used here are still below the threshold density for this transition [21].

In order to investigate timescales longer than the temporal separation between two pulses, we use an electro-optical modulator to gate the nonresonant pump beam. The gate operates at a repetition rate of 100 kHz and opens for 90 or 103 ns, which creates pulse trains of seven or eight full consecutive pulses. We set the intensity of the probe laser to an intensity in the middle of the upper branch of the bistability curve as indicated by the blue dot in Fig. 1(a) and record the time-resolved change of its relative transmission with respect to the nonresonant pump pulses. Figure 2 shows a typical trace of the relative transmission. Shortly after a pulse arrives on the sample, the probe transmission diminishes significantly and slowly increases again afterwards. Surprisingly, we find that the relative transmission does not fully recover until the next pulse arrives. Instead, the suppression builds up quickly over the course of the first four pulses. Afterwards, the peak suppression continues to increase slowly with every additional pulse. After the last pulse of the train has arrived on the sample, the transmission slowly recovers back to the initial value on a long timescale of tens of nanoseconds.

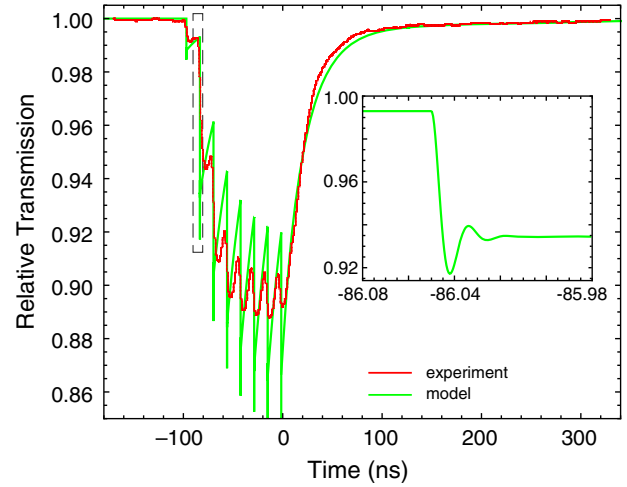


FIG. 2. Relative transmission intensity resolved in time. The gate consists of  $n = 7$  pulses. Red and green curves correspond to the experiment and model, respectively. The slow component shows an exponential decay on a timescale of 22 ns, while the inset shows fast polariton dynamics on the picosecond scale corresponding to the schematic dashed frame in the main figure. The cw pump power corresponds to blue dots in Fig. 1.

As the reduced transmission translates to a spectral shift of the lower polariton mode, these results raise questions about the nature of the carriers causing this shift. While there have been numerous studies on the dynamics of polariton condensates after nonresonant excitation, the focus has so far been on bright excitations. Free carriers may relax and form bright excitonlike polaritons at a large wave vector, which in turn relax down the polariton dispersion via spontaneous or stimulated scattering until they reach the ground state and join the condensate. Both the changes in population dynamics and the presence of free carriers will result in changes of the relative transmission, but they will do so on the short timescale required for carriers to form polaritons, reach the ground state, and leave the cavity. Both are typically on the order of tens of picoseconds [23]. Even considering a possible slow-down of relaxation at small carrier densities, an upper limit for this timescale is given by the bright exciton lifetime. For high-quality quantum wells, it may be as short as tens of picoseconds, but, even for low-quality structures, it will usually not exceed the bulk value of about 1 ns [24]. Therefore, bright carriers fail to explain the long timescale seen in the experiment. This suggests that optically dark excitations play a significant role for long times after nonresonant excitation.

We reproduce the full set of experimental observations with the use of a rate equation model accounting for the long-living reservoir of dark excitons that creates a repulsive potential responsible for the blueshift of the polariton condensate energy. We apply this model to the regime of quasiresonant cw optical excitation, where the bistability curve shown in Fig. 1(a) has been measured, as well as to

the regime of pulsed excitation where the memory effect has been detected, as Fig. 2 shows. We model the dynamics of the system by solving the Gross-Pitaevskii equations for the polariton condensate wave function  $\Psi$  coupled to the rate equations for the occupation numbers of the incoherent reservoir of optically inactive excitons,  $N_X$ :

$$i\hbar d_t \Psi = [-\delta_p + V_b(t) - i\hbar\gamma/2]\Psi + f, \quad (1)$$

$$d_t N_X = P(t) + \beta|f|^2 - \gamma_X N_X. \quad (2)$$

In Eq. (1),  $\delta_p$  is responsible for the detuning of the resonant pump energy from the bare lower polariton energy, which we choose as a reference.  $V_b(t) = g|\Psi|^2 + g_X N_X$  describes the blueshift of the polariton energy due to the intra-condensate polariton interactions and the interaction with the reservoir excitons;  $g$  and  $g_X$  are the corresponding interaction constants.  $f$  is the amplitude of the resonant cw pump.  $\gamma$  is the polariton relaxation rate. Equation (2) is the rate equation for inactive dark reservoir excitons. To take into account filling of the reservoir under the resonant pumping, we introduce the term  $\beta|f|^2$ .  $\beta$  is the dimensional reservoir response constant. The reservoir is also pumped incoherently by the modulated-in-time optical pump  $P(t)$ . The exciton reservoir relaxes at a rate of  $\gamma_X$ .

Under solely resonant pumping, when one assumes  $P = 0$ , the system has been extensively considered for bistability and related effects [15,25–27]. Following Ref. [26], within the one-mode approximation  $\Psi = \psi_p e^{-iE_p t/\hbar}$ , for the driven cavity polariton mode  $\psi_p$ , we obtain

$$|\psi_p|^2 = |f|^2/\theta, \quad (3)$$

where  $\theta = (\delta_p - g|\psi_p|^2 - g_X\beta|f|^2/\gamma_X)^2 + (\hbar\gamma/2)^2$ . The calculated transmission intensity through the structure is given by

$$T \propto |\psi_p|^2/\theta. \quad (4)$$

Figure 1(b) shows the transmission  $T$  as a function of the cw resonant pump power  $|f|^2$ . The parameters used for modeling are given in Ref. [28]. Two branches (solid) corresponding to stable solutions of Eq. (3) nicely qualitatively reproduce the experimental dependence for the transmission shown in Fig. 1(a). The decay in the transmission intensity of the upper hysteresis branch is due to the blueshift of the cavity polariton energy from the pump energy. The blueshift is caused by polariton interactions with the dark exciton reservoir, which may be populated even in the presence of only the resonant pumping in the positive detuning regime. This model is aimed at capturing the essential role of dark excitons in cw and pulsed transmission experiments. It deliberately neglects various additional effects such as spin-anisotropic interactions,

cavity anisotropies, scattering from the condensate towards the reservoir, and nonlinear loss due to biexciton formation [18,29,30].

To model the transmission dynamics, we solve Eqs. (1) and (2) numerically in the presence of the nonresonant optical gate. We take the latter as a train of subpicosecond Gaussian pulses in the form  $P(t) = \sum_{j=0}^{n-1} P_0 \exp[-(t - j/\nu - t_0)^2/w^2]$ , where  $n$  is the number of pulses in one train,  $\nu$  is the pulse repetition rate in one train,  $t_0$  is the time of arrival of the first pulse peak, and  $w$  is a single pulse duration. The green curve in Fig. 2 shows the transmission variation in time in the presence of the optical gate of  $n = 7$  pulses. To take into account noninstantaneous opening of the gate, we assume that an additional pulse enters the system prior to the main train. The pulse possesses an energy of one-tenth of the energy of subsequent pulses. The simulated slow dynamics at the nanosecond scale fully reproduces the measurements. The inset in Fig. 2 shows fast dynamics on the scale of tens of picoseconds. It reflects the population relaxation after the pulse arrival; see also [31]. The monotonic region after the arrival of the last pulse in Fig. 2 allows us to estimate the lifetime of dark excitons as  $1/\gamma_X \approx 22$  ns; see Supplemental Material [21] for the details of the estimation. Based on the simulations in Fig. 2, we are able to estimate the blueshift provided by the train of seven pulses of a given energy as about  $40 \mu\text{eV}$  achieved at the dark exciton density of about  $5 \times 10^8 \text{ cm}^{-2}$ .

One can see that in both cw and pulsed excitation cases the model captures the essential manifestations of the dark exciton reservoir. Namely, in Fig. 1(b), we reproduce the characteristic decrease of the transmission signal as a function of the pump power that is a signature of the detuning of the condensate energy from the laser mode energy that is governed by the population of the dark reservoir. In Fig. 2, the model quantitatively reproduces the dependence of the transmission modulation induced by laser pulses on the reservoir density created by previous pulses.

Several types of excitations could be at the heart of the long-lived line shifts. Parity-forbidden and spatially indirect excitons are unlikely candidates. In addition, coherent multidimensional spectroscopy has demonstrated that they usually show some weak coupling to bright states, which limits their lifetime drastically [32]. The same holds true for the nominally dark  $J_z = \pm 1$  antisymmetric polariton states that form in microcavity structures containing more than one quantum well. Because of coupling with leaky modes, their lifetime is reduced drastically to values below 1 ns [33]. These states form a possible decay channel for dark states, but, as they are delocalized, the overlap integral between dark excitons and these states is expected to be small. For biexcitons, also much shorter lifetimes are expected [18]. Two kinds of dark excitations should be retained as candidates for the observed dark carrier

population. First, spin-forbidden dark excitons with an exciton spin projection of  $J_z = \pm 2$  may form under nonresonant excitation. These excitations can decay only nonradiatively or by spin relaxation towards a bright state. Second, spin-allowed carriers with  $J_z = \pm 1$  may form at large wave vectors  $k_{\parallel}$ . If their wave vector exceeds that of light inside the medium, they also cannot couple to light fields and are thus optically dark. A closer look at the typical relaxation processes already sheds some light on the processes taking place.

In quantum wells not embedded inside a microcavity, the spin relaxation time between dark  $J_z = \pm 2$  excitons and bright  $J_z = \pm 1$  excitons is governed by the short-range exchange interaction between excitons [34], which causes an energy splitting of about  $80 \mu\text{eV}$  between the bright and dark states with dark states being at lower energy [35]. This splitting results in a spin relaxation timescale of about 80 ps. For quantum wells embedded into a microcavity, the situation changes drastically. In the strong coupling regime, the light-matter interaction shifts the bright state to lower energies by a value given by half the Rabi energy. As this splitting is significantly larger than the splitting in bare quantum wells, also the spin relaxation time by exciton-exciton interaction is expected to become much longer at small  $k_{\parallel}$ . However, as the splitting depends on  $k_{\parallel}$  and due to symmetry reasons, mixing of bright and dark states occurs at  $k_{\parallel} \neq 0$  [36], especially in the bottleneck region [37]. Therefore, it is expected that primarily dark excitons with  $J_z = \pm 2$  at  $k_{\parallel} = 0$  will show a drastically enhanced lifetime. Because of the large value of the Rabi splitting, it is expected that relaxation will mostly occur via phonons to bright polariton states in the bottleneck region of the dispersion or with some small probability towards the antisymmetric dark polariton states. Both processes will not depend strongly on the dark exciton density. For  $J_z = \pm 1$  excitons at a large wave vector, momentum and energy relaxation towards the optically active region is supposed to be the most important relaxation channel. Thus, exciton-exciton scattering should play a significant role, and some kind of density dependence is expected.

In order to gain some insight on these scenarios and also to estimate the magnitude of suppression of transmission we are able to achieve, we compared the dynamics of the suppression for different nonresonant pump powers as shown in Fig. 3. First, indeed the suppression can be enhanced by pumping more strongly. The transmission can be reduced to values below 15% of its initial value. Second, there is no apparent dependence of the relaxation timescale on the nonresonant pump intensity. Accordingly, although the microscopic nature of the dark carriers in our experiment is not known unambiguously, we cautiously suggest that spin-forbidden dark excitons at low momentum are the most likely candidates. Additionally, we also found compelling evidence that the interaction between them and bright polaritons is repulsive: When driven below the

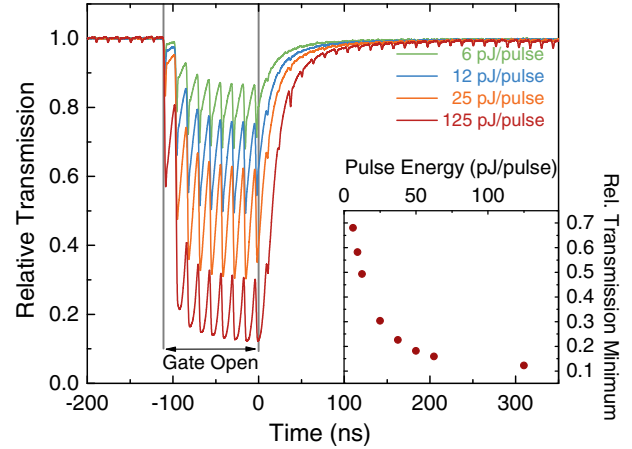


FIG. 3. The relative transmission intensity resolved in time after the arrival of a train of eight pulses for different pumping energies. The dashed lines represent the temporal region where the gate is open and the system is excited nonresonantly with a pulse repetition rate of  $\nu = 75$  MHz. The periodic signal at large pump energies arises due to the finite extinction ratio of about 1:100 of the intensity modulator. Inset: Circles represent the minimum value of the relative transmission for different pumping energies.

nonlinear threshold, additional pulsed nonresonant excitation significantly enhances the transmission, which is a signature of an interaction-induced blueshift of the polariton mode [21].

In summary, we have demonstrated that a narrow polariton mode may be utilized as a sensitive probe for the presence of dark excitations in a semiconductor system. We found that these carriers have a surprisingly long lifetime of more than 20 ns. Besides the possibility to unveil the dynamics of optically dark excitations, which are difficult to address otherwise, our result has several important implications. First, it demonstrates the possibility to optically imprint potential landscapes for polaritons that last 3 orders of magnitude longer than the polariton lifetime in the system. This provides interesting perspectives for functional polariton circuits and classical polariton simulators [38–42]. Resonant injection of dark excitons via two-photon absorption [36,43,44] might provide the means to create tailored optical potentials without perturbing relaxation dynamics. Finally, typical pulsed excitation experiments on polariton systems employ lasers with a pulse separation of about 13 ns. The existence of dark excitations with a lifetime longer than that implies that the standard assumption that the system is completely empty before an excitation pulse arrives is not tenable, which is of high importance for studies of condensate formation.

We gratefully acknowledge support from the DFG in the framework of TRR 160 within project B7 (ID 269934647) and the Russian Foundation for Basic Research (RFBR, Grant No. 19-52-12032). E. S. S. acknowledges support

from RFBR Grants No. 16-32-60104 and No. 17-52-10006. A. V. K. acknowledges financial support from St-Petersburg State University within research Grant No. 11.34.2.2012 (ID 28874264) and partial support from the Royal Society International Exchange Grant No. IEC/R2/170227. C. S. acknowledges support from the DFG in the framework of Project No. SCHN1376/3-1.

- 
- [1] E. Malic, M. Selig, M. Feierabend, S. Brem, D. Christiansen, F. Wendler, A. Knorr, and G. Berghäuser, *Phys. Rev. Mater.* **2**, 014002 (2018).
- [2] N. Lundt, S. Stoll, P. Nagler, A. Nalitov, S. Klemmt, S. Betzold, J. Goddard, E. Frieling, A. V. Kavokin, C. Schüller, T. Korn, S. Höfling, and C. Schneider, *Phys. Rev. B* **96**, 241403 (2017).
- [3] G. Wang, C. Robert, M. M. Glazov, F. Cadiz, E. Courtade, T. Amand, D. Lagarde, T. Taniguchi, K. Watanabe, B. Urbaszek, and X. Marie, *Phys. Rev. Lett.* **119**, 047401 (2017).
- [4] S. Bode, C. C. Quentmeier, P.-N. Liao, N. Hafı, T. Barros, L. Wilk, F. Bittner, and P. J. Walla, *Proc. Natl. Acad. Sci. U.S.A.* **106**, 12311 (2009).
- [5] M. Nirmal, D. J. Norris, M. Kuno, M. G. Bawendi, A. L. Efros, and M. Rosen, *Phys. Rev. Lett.* **75**, 3728 (1995).
- [6] A. L. Efros, M. Rosen, M. Kuno, M. Nirmal, D. J. Norris, and M. Bawendi, *Phys. Rev. B* **54**, 4843 (1996).
- [7] H. Kurtze, D. R. Yakovlev, D. Reuter, A. D. Wieck, and M. Bayer, *Phys. Rev. B* **85**, 195303 (2012).
- [8] I. Schwartz, D. Cogan, E. R. Schmidgall, Y. Don, L. Gantz, O. Kenneth, N. H. Lindner, and D. Gershoni, *Science* **354**, 434 (2016).
- [9] D. Bajoni, E. Semenova, A. Lemaître, S. Bouchoule, E. Wertz, P. Senellart, S. Barbay, R. Kuszelewicz, and J. Bloch, *Phys. Rev. Lett.* **101**, 266402 (2008).
- [10] M. Amthor, T. C. H. Liew, C. Metzger, S. Brodbeck, L. Worschech, M. Kamp, I. A. Shelykh, A. V. Kavokin, C. Schneider, and S. Höfling, *Phys. Rev. B* **91**, 081404 (2015).
- [11] L. Pickup, K. Kalinin, A. Askitopoulos, Z. Hatzopoulos, P. G. Savvidis, N. G. Berloff, and P. G. Lagoudakis, *Phys. Rev. Lett.* **120**, 225301 (2018).
- [12] O. Kyriienko, E. A. Ostrovskaya, O. A. Egorov, I. A. Shelykh, and T. C. H. Liew, *Phys. Rev. B* **90**, 125407 (2014).
- [13] N. A. Gippius, I. A. Shelykh, D. D. Solnyshkov, S. S. Gavrilov, Y. G. Rubo, A. V. Kavokin, S. G. Tikhodeev, and G. Malpuech, *Phys. Rev. Lett.* **98**, 236401 (2007).
- [14] J.-Y. Lien, Y.-N. Chen, N. Ishida, H.-B. Chen, C.-C. Hwang, and F. Nori, *Phys. Rev. B* **91**, 024511 (2015).
- [15] A. Baas, J. P. Karr, H. Eleuch, and E. Giacobino, *Phys. Rev. A* **69**, 023809 (2004).
- [16] M. Vladimirova, S. Cronenberger, D. Scalbert, K. V. Kavokin, A. Miard, A. Lemaître, J. Bloch, D. Solnyshkov, G. Malpuech, and A. V. Kavokin, *Phys. Rev. B* **82**, 075301 (2010).
- [17] C. Ouellet-Plamondon, G. Sallen, F. Morier-Genoud, D. Y. Oberli, M. T. Portella-Oberli, and B. Deveaud, *Phys. Rev. B* **95**, 085302 (2017).
- [18] M. Wouters, T. K. Paraiso, Y. Léger, R. Cerna, F. Morier-Genoud, M. T. Portella-Oberli, and B. Deveaud-Plédran, *Phys. Rev. B* **87**, 045303 (2013).
- [19] J. Schmutzler, T. Kazimierczuk, O. Bayraktar, M. Abmann, M. Bayer, S. Brodbeck, M. Kamp, C. Schneider, and S. Höfling, *Phys. Rev. B* **89**, 115119 (2014).
- [20] J.-M. Ménard, C. Poellmann, M. Porer, U. Leierseder, E. Galopin, A. Lemaître, A. Amo, J. Bloch, and R. Huber, *Nat. Commun.* **5**, 4648 (2014).
- [21] See Supplemental Material at <http://link.aps.org/supplemental/10.1103/PhysRevLett.122.047403>, including Ref. [22] for a full discussion of the dark exciton lifetime, the weak coupling transition, and the polariton-exciton interaction.
- [22] D. Ballarini, D. Sanvitto, A. Amo, L. Viña, M. Wouters, I. Carusotto, A. Lemaître, and J. Bloch, *Phys. Rev. Lett.* **102**, 056402 (2009).
- [23] H. Deng, H. Haug, and Y. Yamamoto, *Rev. Mod. Phys.* **82**, 1489 (2010).
- [24] B. Deveaud, F. Clérot, N. Roy, K. Satzke, B. Sermage, and D. S. Katzer, *Phys. Rev. Lett.* **67**, 2355 (1991).
- [25] M. Wouters and I. Carusotto, *Phys. Rev. B* **75**, 075332 (2007).
- [26] S. S. Gavrilov, *Phys. Rev. B* **90**, 205303 (2014).
- [27] E. Cancellieri, A. Hayat, A. M. Steinberg, E. Giacobino, and A. Bramati, *Phys. Rev. Lett.* **112**, 053601 (2014).
- [28] The polariton energy detuning is  $\delta_p = 650 \mu\text{eV}$ . The interaction coefficient is  $g = g_X/3 = 0.6 \mu\text{eV}$ . The polariton relaxation rate is  $\gamma = 0.3 \text{ ps}^{-1}$ . The pulse repetition rate is  $\nu^{-1} = 13.3 \text{ ns}$ , and the duration of one pulse is  $w = 200 \text{ fs}$ .
- [29] P. M. Walker, L. Tinkler, B. Royall, D. V. Skryabin, I. Farrer, D. A. Ritchie, M. S. Skolnick, and D. N. Krizhanovskii, *Phys. Rev. Lett.* **119**, 097403 (2017).
- [30] S. S. Gavrilov, A. S. Brichkin, A. A. Dorodnyi, S. G. Tikhodeev, N. A. Gippius, and V. D. Kulakovskii, *JETP Lett.* **92**, 171 (2010).
- [31] R. Cerna, Y. Léger, T. K. Paraiso, M. Wouters, F. Morier-Genoud, M. T. Portella-Oberli, and B. Deveaud, *Nat. Commun.* **4**, 2008 (2013).
- [32] J. O. Tollerud, S. T. Cundiff, and J. A. Davis, *Phys. Rev. Lett.* **117**, 097401 (2016).
- [33] M. Richard, R. Romestain, R. Andr, and L. S. Dang, *Appl. Phys. Lett.* **86**, 071916 (2005).
- [34] D. W. Snoke, W. W. Rühle, K. Köhler, and K. Ploog, *Phys. Rev. B* **55**, 13789 (1997).
- [35] L. Viña, *J. Phys. Condens. Matter* **11**, 5929 (1999).
- [36] C. Gautham, M. Steger, D. Snoke, K. West, and L. Pfeiffer, *Optica* **4**, 118 (2017).
- [37] I. Shelykh, L. Viña, A. Kavokin, N. Galkin, G. Malpuech, and R. Andrè, *Solid State Commun.* **135**, 1 (2005).
- [38] N. G. Berloff, M. Silva, K. Kalinin, A. Askitopoulos, J. D. Töpfer, P. Cilibrizzi, W. Langbein, and P. G. Lagoudakis, *Nat. Mater.* **16**, 1120 (2017).
- [39] G. Tosi, G. Christmann, N. G. Berloff, P. Tsotsis, T. Gao, Z. Hatzopoulos, P. G. Savvidis, and J. J. Baumberg, *Nat. Phys.* **8**, 190 (2012).
- [40] M. Abmann, F. Veit, M. Bayer, A. Löffler, S. Höfling, M. Kamp, and A. Forchel, *Phys. Rev. B* **85**, 155320 (2012).

- [41] A. Askitopoulos, A. V. Nalitov, E. S. Sedov, L. Pickup, E. D. Cherotchenko, Z. Hatzopoulos, P. G. Savvidis, A. V. Kavokin, and P. G. Lagoudakis, *Phys. Rev. B* **97**, 235303 (2018).
- [42] J. Schmutzler, P. Lewandowski, M. Aßmann, D. Niemietz, S. Schumacher, M. Kamp, C. Schneider, S. Höfling, and M. Bayer, *Phys. Rev. B* **91**, 195308 (2015).
- [43] G. Leménager, F. Pisanello, J. Bloch, A. Kavokin, A. Amo, A. Lemaitre, E. Galopin, I. Sagnes, M. D. Vittorio, E. Giacobino, and A. Bramati, *Opt. Lett.* **39**, 307 (2014).
- [44] J. Schmutzler, M. Aßmann, T. Czerniuk, M. Kamp, C. Schneider, S. Höfling, and M. Bayer, *Phys. Rev. B* **90**, 075103 (2014).